

Benchmarking CNN-based Models against Transformer-based Models for Abdominal Multi-Organ Segmentation on the RATIC Dataset

Lukas Bayer¹, Sheethal Bhat¹, Andreas Maier¹

¹Pattern Recognition Lab Friedrich-Alexander-Universität Erlangen-Nürnberg
lukas.bayer@fau.de

Abstract. Accurate multi-organ segmentation in abdominal CT scans is essential for computer-aided diagnosis and treatment. While convolutional neural networks (CNNs) have long been the standard approach in medical image segmentation, transformer-based architectures have recently gained attention due to their ability to model long-range dependencies. In this study, we systematically benchmark the three hybrid transformer-based models UNETR, SwinUNETR, and UNETR++ against a strong CNN baseline, SegResNet, for volumetric multi-organ segmentation on the heterogeneous RATIC dataset. The dataset comprises 206 annotated CT scans from 23 institutions worldwide, covering five abdominal organs. All models were trained and evaluated under identical preprocessing and training conditions using the Dice Similarity Coefficient (DSC) as the primary metric. The results show that the CNN-based SegResNet achieves the highest overall performance, outperforming all hybrid transformer-based models across all organs. Among the transformer-based approaches, UNETR++ delivers the most competitive results, while UNETR demonstrates notably faster convergence with fewer training iterations. These findings suggest that, for small- to medium-sized heterogeneous datasets, well-optimized CNN architectures remain highly competitive and may outperform hybrid transformer-based designs.
Code: https://github.com/lukas-FAU/medical_image_segmentation_benchmarking_paper

Keywords: Abdominal Multi-Organ Segmentation, RATIC Dataset, Benchmarking, UNETR, SwinUNETR, UNETR++, SegResNet

1 Introduction

Abdominal multi-organ segmentation is a cornerstone of modern digital medicine, transforming static pixels from CT scans into dynamic, 3D anatomical maps.

Over the past decade, convolutional neural networks (CNNs), in particular U-Net-based [1] architectures, have become the de facto standard for medical image segmentation due to their strong inductive bias toward local spatial context and their data efficiency.

More recently, transformer-based [2] models have been introduced to overcome the limited receptive field of convolutions by modeling long-range dependencies through self-attention. Hybrid approaches such as UNETR [3], SwinUNETR [4], and UNETR++ [5] combine transformer encoders with convolutional decoders and have reported competitive or superior results on abdominal multi-organ segmentation tasks.

However, benchmarking between CNN-based and transformer-based models is frequently confounded by the practice of evaluating baselines while simultaneously proposing a new architecture. Therefore reported performance metrics for a single architecture that is used as baseline often exhibits a significant inter-publication variance. For instance, the UNETR [3] model which is commonly used as a baseline yields reported DSC scores ranging from 0.6888 [6] to 0.8910 [3, 7], with intermediate results of 0.7835 [8], 0.8027 [9], and 0.8129 [10] while trained on the BTCV dataset [11] with comparable hyperparameters. This variance makes it difficult to draw conclusions about the actual performance of architectures on abdominal multi-organ segmentation tasks. This also complicates a systematic comparison of the performance of CNN-based and transformer-based models. Therefore independent performance benchmarks are important to provide a fair and comprehensive comparison of different architectures under identical conditions.

While several meta-analyses [12, 13] evaluating the performance of transformer-based models compared to CNN-based models exist, the field lacks a comprehensive comparison with independent benchmarks. To the best of our knowledge, currently only one independent benchmark has been published comparing the segmentation performance of CNN-based and transformer-based models on abdominal CT datasets. This study [14] by Isensee et al. has shown that CNN-based models systematically outperform transformer-based models in abdominal multi-organ segmentation tasks when trained on small datasets of 50 scans while certain architectures achieve almost the same accuracy when trained on larger datasets with over 500 scans. However, while including 12 CNN-based models it only benchmarks 4 transformer-based models, leaving out some transformer-based architectures like UNETR [3] and UNETR++ [5] that reported competitive performance in their original publications. Furthermore, it did not include medium-sized datasets of around 200 scans. Since it is often claimed that the size of the training dataset is a crucial factor for the performance of transformer-based models [2], it is important to evaluate the performance of these models on medium-sized datasets as well.

Therefore in this work, we systematically benchmark the three hybrid transformer-based architectures UNETR, SwinUNETR and UNETR++ against a strong CNN baseline, SegResNet, for abdominal multi-organ segmentation on the medium-sized and heterogeneous RATIC dataset. By evaluating segmentation accuracy, convergence behavior across heterogeneous CT scans, we aim to provide insights into whether transformer-based designs offer tangible advantages over well-optimized CNNs in this setting.

2 Materials and Methods

2.1 Dataset details

For this benchmark we used the RATIC dataset [15], which was published by the Radiological Society of North America (RSNA) in 2023. The dataset provides in total 206 pixel-level segmentation labels of the liver, spleen, left kidney, right kidney, and bowel in Neuroimaging Informatics Technology Initiative (NIFTI) format. The labels were created by a nnU-Net model [16] trained on the TotalSegmentator dataset [17] and manually corrected by medical experts. The CT images are provided in Digital Imaging and Communications in Medicine (DICOM) format. Each scan has a size of 512x512 pixels in the axial plane, while the number of slices in the z-direction varies between 50 and 300.

We split the dataset into a training set of 144 scans, a validation set of 41 scans and a test set of 21 scans. Figure 1 shows the class-wise distribution of the training, validation and test set. The dataset is imbalanced, with larger organs like the bowel and the liver appearing more frequently than smaller organs like the kidneys or the spleen.

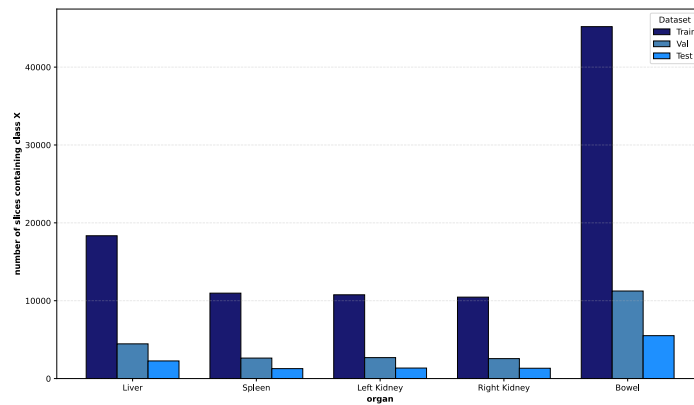


Fig. 1. Class wise distribution for train, test and validation dataset

Before training, the CT scans and labels were preprocessed. The following steps were performed:

Orientation. The NIFTI files for the labels use a Right-Anterior-Superior (RAS) coordinate system. However, the CT images, which are in DICOM format, use a Left-Posterior-Superior (LPS) coordinate system. Therefore, the CT images were reoriented to match the RAS system of the labels.

Spacing. The RATIC dataset [15] contains CT scans from 23 institutions across 14 countries and six continents. Therefore, it can be assumed that the scans were acquired using different CT scanners with varying acquisition protocols. As a result, the voxel spacing can vary significantly between scans. To ensure that all images have the same voxel spacing, we resampled all images and segmentations to an isotropic spacing of $1\text{mm} \times 1\text{mm} \times 1\text{mm}$.

Normalization. While the NIfTI files already have an intensity scale in the range from 0 to 1, as it is needed for training neural networks, the DICOM files in the RATIC dataset stores the intensity values in a range from -150 to 250. Therefore, we normalized the intensity values of the CT images to the range $[0, 1]$.

Class Imbalance. For training we did not use the whole 3D volume of the CT scans, but randomly sampled patches of size $96 \times 96 \times 96$ voxels. However, due to the varying sizes of the organs and the high amount of background voxels, there is a significant class imbalance. To address this, we used a patch sampling strategy that ensures that patches containing smaller organs are sampled more frequently. We used the following sampling ratios: $[1:1:2:2:2:1]$ for [background, liver, left kidney, right kidney, spleen, bowel]. This means that patches containing the kidneys or spleen are sampled twice as often as patches containing only background, liver or bowel.

We also tried a similar ratio for the weighting of the loss function during training, but this made the training less stable while not leading to an improvement in performance.

A different approach we tested was to increase the size of the patches to $128 \times 128 \times 128$ voxels. This way, each patch contains more context information and the organs occupy a larger portion of the patch. However, due to the limited GPU memory, this only allowed for a batch size of 1 during training, which made the training less stable and did not lead to an improvement in performance.

Generalization. To improve the generalization of the models, we used random flips along all three axes as well as random rotations of 90, 180 and 270 degrees during training. We also applied random intensity scaling and shifting to the input images.

2.2 The Segmentation Models

This assessment evaluates four state-of-the-art models for medical image segmentation, comprising one CNN-based model and three hybrid models which use a transformer-based encoder combined with a CNN-based decoder.

UNETR. UNETR [3] is a U-Net [1] style segmentation model. It was one of the first architectures which successfully completely replaced the encoder of a U-Net with a Vision Transformer (ViT) [18]. In the encoder, the 3D input volume is split into non-overlapping patches, which are then flattened and projected into a 1D sequence of embeddings. Then positional embeddings are added to the tokens and the sequence is passed through multiple transformer layers. Through skip connections feature maps

are extracted from layers 3, 6, 9 and 12 of the transformer encoder. The decoder remains convolutional. It is a hierarchical CNN that upsamples the feature map extracted by the transformer encoder's last layer and combines it with the feature maps that were extracted from different encoder stages via skip connections. Finally, when the decoder reaches the original input resolution, a $1 \times 1 \times 1$ convolution is used to project the features into the desired number of output classes.

Since it uses transformer blocks in the encoder, UNETR is able to capture long-range dependencies and global context information. However, it also has a large number of parameters and requires a larger amount of training data to achieve good performance.

SwinUNETR. SwinUNETR [4] is also a U-Net style architecture. Similar to UNETR, it replaces the encoder of a U-Net with a transformer-based architecture. However, instead of using a ViT as encoder, it uses a Swin Transformer [19]. The Swin Transformer uses shifted windows to compute self-attention locally, which reduces the computational complexity compared to global self-attention. The Swin Transformer encoder consists of four stages, each reducing the resolution of the input by a factor of two. Feature maps are extracted from each of the four stages and passed to the convolutional decoder via skip connections. The decoder is similar to the one used in UNETR. It progressively upsamples the feature maps and combines them with the corresponding encoder features. A final $1 \times 1 \times 1$ convolution is used to produce the segmentation output.

The Shifted window attention reduces complexity from quadratic to linear relative to image size, promising an increase in training speed.

UNETR++. UNETR++ [5] is an improved version of UNETR. It retains the overall architecture of UNETR, but uses several enhancements to improve performance. While UNETR uses pure vision transformer blocks in the encoder, UNETR++ uses a hybrid approach that combines convolutional layers with transformer blocks. First the input is downsampled before passing through an efficient paired-attention (EPA) block. The EPA block computes two types of attention: spatial attention and channel attention, which are then combined to produce the output feature map. This allows the model to capture both local and global features more effectively. Additionally, UNETR++ uses a decoder that is symmetric to the encoder, with skip connections between corresponding encoder and decoder layers. This helps to preserve spatial information and improve segmentation accuracy. Like UNETR, a final $1 \times 1 \times 1$ convolution is used to produce the segmentation output.

UNETR++ is designed to improve efficiency and accuracy compared to UNETR. However, it also has a larger number of parameters and may require more training data to achieve good performance.

SegResNet. SegResNet [20] is a CNN-based architecture that extends the U-Net design by adding residual blocks. Unlike standard symmetric U-Net, the encoder is significantly larger and deeper than the decoder. It uses ResNet-style blocks where each block consists of Group Normalization, a ReLU activation, 3D convolutions

and a skip connection. The decoder uses 3D bilinear upsampling followed by a $1 \times 1 \times 1$ convolutions to reduce the number of feature channels before concatenating them with skip connections from the encoder. The SegResNet architecture proposed in the original paper also uses a variational autoencoder (VAE) branch to regularize the encoder. However, the implementation we use for this benchmark does not include the VAE branch.

SegResNet is a simple and robust architecture that works well with small sized datasets. However, since it is a CNN-based architecture, it may have limitations in capturing long-range dependencies.

We chose these four models for our benchmark because they all are commonly used when evaluating new architectures. Therefore, it is important to evaluate their performance independently to provide a fair comparison for future studies that use these models as baselines.

2.3 Evaluation Metrics

For evaluating the segmentation performance of the models, we calculated the Dice Similarity Coefficient (DSC) [21] for each organ. Then, We computed the mean DSC across all organs to obtain an overall performance metric for each model. The DSC is defined as:

$$DSC = \frac{2|A \cap B|}{|A| + |B|} \quad (1)$$

where A is the set of voxels in the predicted segmentation and B is the set of voxels in the ground truth segmentation. The DSC ranges from 0 to 1, with 1 indicating perfect overlap between the predicted and ground truth segmentations.

3 Results

3.1 Implementation Details

All models except UNETR++ as well as the preprocessing, training, testing and validation steps were implemented using the MONAI [22] and PyTorch [23] Framework.

For UNETR we used a feature size of 16, the dimension of the hidden layer was 798, the dimension of the feedforward layer was 3072 and we used 12 attention heads.

For SwinUNETR we used a feature size for 48, respectively the hidden layer dimensions were 48, 96, 192, 384 for the four stages of the Swin Transformer encoder and we used 3, 6, 12, 24 attention heads for the four stages.

For SegResNet we used a initial filter size of 16 and the probability for dropout was 0.2. The number of downsample blocks in the four encoder layers were 1, 2, 2, 4 and the number of upsample blocks in the three decoder layers were 1, 1, 1. The SegResNet implementation we use for this benchmark does not include the VAE branch.

For UNETR++ we used the official implementation provided by the authors [5] via this GitHub repository: https://github.com/Amshaker/unetr_plus_plus. We used a feature size of 16 as well as 4 attention heads and 3 EPA blocks on each of the four stages. The number of channels on each stage were 32, 64, 128 and 256.

We figured out that the hyperparameters as described above worked best for our dataset. A visualization of the architectures as they were used can be found in the appendix.

All models were trained on the same hardware, which consisted of a single NVIDIA A100 GPU with 40GB of VRAM.

3.2 Results and Discussion

Table 1 presents the results of the quantitative evaluation of the four models on the RATIC test set. The table shows the mean DSC for each organ as well as the average DSC across all organs.

The CNN-based model SegResNet outperforms the three transformer-based models UNETR, SwinUNETR and UNETR++ in terms of average DSC. It also achieves the highest DSC for each individual organ. Among the transformer-based models, UNETR++ performs best. It demonstrates competitive performance, especially for the left and right kidney as well as the liver, while slightly underperforming on segmenting the spleen and bowel. While UNETR shows a slightly worse but still strong performance, SwinUNETR performs significantly worse than the other models. SwinUNETR is not just severely underperforming on segmenting the left kidney but also shows a significant drop in performance for all organs except the liver. This leads to a significantly lower average DSC for SwinUNETR compared to the others.

These findings indicate that Transformer-based models like UNETR, SwinUNETR and UNETER++ that previously claimed to outperform CNN-based models like U-Net or SegResNet [3–5] on segmentation tasks, do not necessarily achieve better performance than a well-optimized CNN-based model like SegResNet when trained on a medium-sized dataset of 144 scans. We assume that the reason for this is that CNNs possess a strong inductive bias toward local spatial context [2]. This makes them inherently more data-efficient than transformer-based models.

These results support the findings of the study by Isensee et al. [14] which reports that when CNN-based architectures are properly configured, they often perform as well as, or better than, newer Transformer-based models. However, when comparing the performance of UNETR++ which was not part of the study by Isensee et al. and SegResNet, we see that the performance gap is minor with only 1.1%. Since the success of a model is often influenced by the specific dataset, its preprocessing as well as the hyperparameters used during training, this margin is too small to draw a general conclusion about the superiority of one architecture over the other. Therefore we assume that a well-chosen and optimized transformer-based architecture can at least achieve similar performance as a CNN-based architecture.

With the exception of SwinUNETR’s outlier regarding the left kidney, table 1 also shows that both CNN-based and transformer-based models achieve better

performance on organs like liver or kidneys compared to the performance on spleen, bowel. Therefore transformer-based as well as CNN-based models seem to have similar difficulties in learning the structures of non-uniform, more complex and disjointed organs like the bowel, while they perform better on more uniform and compact organs like the liver or kidneys. This can also be observed in Figure 2, which shows a qualitative comparison of the segmentation results of the four models on a test scan from the RATIC dataset.

	Spleen	Right Kidney	Left Kidney	Liver	Bowel	Average
UNETR	0.863	0.936	0.949	0.958	0.886	0.918
SwinUNETR	0.811	0.876	0.698	0.933	0.826	0.829
UNETR++	0.907	0.945	0.959	0.963	0.902	0.934
SegResNet	0.919	0.954	0.960	0.970	0.923	0.945

Tab. 1. Quantitative comparisons of segmentation performance on RATIC [24] test set. The table shows the mean Dice Similarity Coefficient (DSC) for Spleen, Right Kidney, Left Kidney and Liver, Bowel and the average DSC across all 5 organs in the RATIC dataset. The top section containing the transformer-based models and the bottom section containing the CNN-based model.

Table 2 shows the number of training iterations needed for each model to achieve the results. The number of iterations is the total number of batches processed over the entire training period. The batch size was 6 for all models.

The table shows that there is no significant difference between the CNN-based model and most transformer-based models. However, UNETR++ requires only about half the number of iterations compared to the other models. This is likely due to the use of "Efficient Paired Attention" (EPA) in UNETR++, which combines spatial and channel attention to capture both local and global features more effectively. This allows UNETR++ to converge faster during training, even though its final performance is slightly lower than SegResNet.

	Iterations
UNETR	10,000
SwinUNETR	10,000
UNETR++	5,000
SegResNet	10,000

Tab. 2. The table shows the number of training iterations needed for each model to achieve the results. The number of iterations is the total number of batches processed over the entire training period. The batch size was 6 for all models.

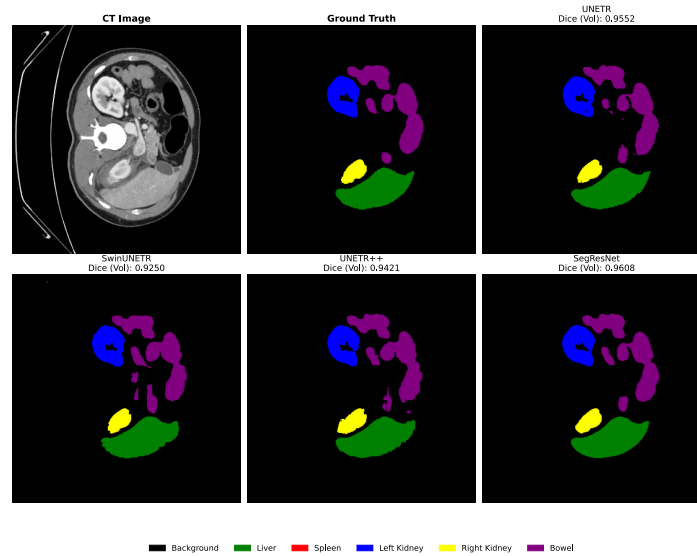


Fig. 2. Qualitative comparison of the performance of UNETR, SwinUNETR, UNETR++ and SegResNet on a test scan from the RATIC dataset. The figure shows the predicted segmentation masks for each model next to the original CT scan. The ground truth segmentation is shown for comparison.

4 Conclusion

Our benchmark demonstrates that the CNN-based model SegResNet outperforms the three transformer-based models UNETR, SwinUNETR and UNETR++ in abdominal multi-organ segmentation on the RATIC dataset. Therefore we conclude that, well-optimized CNN architectures remain highly competitive.

Furthermore our results reveal that the performance claims for abdominal multi-organ segmentation of some transformer-based architectures like SwinUNETR do not hold up when evaluated under independent and identical conditions. Which supports questions raised by Isensee et al. [14] about how currently new architectures are evaluated.

However, our results also show that the performance gap between the best transformer-based model UNETR++ and the CNN-based model SegResNet is minor. Especially when also considering the resources needed for training, the models UNETR++ has an advantage. Therefore we consider certain transformer-based models like UNETR++ to be competitive.

References

1. Ronneberger O, Fischer P, Brox T. U-Net: Convolutional Networks for Biomedical Image Segmentation. CoRR. 2015;abs/1505.04597.

2. Dosovitskiy A, Beyer L, Kolesnikov A, Weissenborn D, Zhai X, Unterthiner T et al. An Image is Worth 16x16 Words: Transformers for Image Recognition at Scale. 2021.
3. Hatamizadeh A, Tang Y, Nath V, Yang D, Myronenko A, Landman B et al. UNETR: Transformers for 3D Medical Image Segmentation. 2021.
4. Hatamizadeh A, Nath V, Tang Y, Yang D, Roth H, Xu D. Swin UNETR: Swin Transformers for Semantic Segmentation of Brain Tumors in MRI Images. 2022.
5. Shaker A, Maaz M, Rasheed H, Khan S, Yang MH, Khan FS. UNETR++: Delving into Efficient and Accurate 3D Medical Image Segmentation. 2024.
6. Chang A, Zeng J, Huang R, Ni D. EM-Net: Efficient Channel and Frequency Learning with Mamba for 3D Medical Image Segmentation. Medical Image Computing and Computer Assisted Intervention – MICCAI 2024. Ed. by Linguraru MG, Dou Q, Feragen A, Giannarou S, Glocker B, Lekadir K et al. Cham: Springer Nature Switzerland, 2024:266–75.
7. Tang Y, Yang D, Li W, Roth HR, Landman B, Xu D et al. Self-Supervised Pre-Training of Swin Transformers for 3D Medical Image Analysis. Proceedings of the IEEE/CVF Conference on Computer Vision and Pattern Recognition (CVPR). 2022:20730–40.
8. Li Q, Tong J, Yang S, Du S. FATUnetr: fully attention Transformer for 3D medical image segmentation. 2024 IEEE International Conference on Mechatronics and Automation (ICMA). 2024:1415–9.
9. Das BK, Singh A, Islam S, Zhao G, Maier A. SegResMamba: An Efficient Architecture for 3D Medical Image Segmentation. 2025.
10. Xing Z, Zhu L, Yu L, Xing Z, Wan L. Hybrid Masked Image Modeling for 3D Medical Image Segmentation. IEEE Journal of Biomedical and Health Informatics. 2024;28(4):2115–25.
11. harrigr. Segmentation Outside the Cranial Vault Challenge. 2015.
12. Takahashi S, Sakaguchi Y, Kouno N, Takasawa K, Ishizu K, Akagi Y et al. Comparison of Vision Transformers and Convolutional Neural Networks in Medical Image Analysis: A Systematic Review. Journal of Medical Systems. 2024;48(1):84.
13. Pu Q, Xi Z, Yin S, Zhao Z, Zhao L. Advantages of transformer and its application for medical image segmentation: a survey. BioMedical Engineering OnLine. 2024;23(1):14.
14. Isensee F, Wald T, Ulrich C, Baumgartner M, Roy S, Maier-Hein K et al. nnU-Net Revisited: A Call for Rigorous Validation in 3D Medical Image Segmentation. Medical Image Computing and Computer Assisted Intervention – MICCAI 2024. Ed. by Linguraru MG, Dou Q, Feragen A, Giannarou S, Glocker B, Lekadir K et al. Cham: Springer Nature Switzerland, 2024:488–98.
15. Rudie JD, Lin HM, Ball RL, Jalal S, Prevedello LM, Nicolaou S et al. The RSNA Abdominal Traumatic Injury CT (RATIC) Dataset. Radiology: Artificial Intelligence. 2024;6(6):e240101.
16. Isensee F, Petersen J, Klein A, Zimmerer D, Jaeger PF, Kohl S et al. nnU-Net: Self-adapting Framework for U-Net-Based Medical Image Segmentation. 2018.
17. Wasserthal J, Breit HC, Meyer MT, Pradella M, Hinck D, Sauter AW et al. TotalSegmentator: Robust Segmentation of 104 Anatomic Structures in CT Images. Radiology: Artificial Intelligence. 2023;5(5).
18. Dosovitskiy A, Beyer L, Kolesnikov A, Weissenborn D, Zhai X, Unterthiner T et al. An Image is Worth 16x16 Words: Transformers for Image Recognition at Scale. CoRR. 2020;abs/2010.11929.
19. Liu Z, Lin Y, Cao Y, Hu H, Wei Y, Zhang Z et al. Swin Transformer: Hierarchical Vision Transformer using Shifted Windows. 2021.

20. Myronenko A. 3D MRI brain tumor segmentation using autoencoder regularization. 2018.
21. Dice LR. Measures of the Amount of Ecologic Association Between Species. *Ecology*. 1945;26(3):297–302.
22. Cardoso MJ, Li W, Brown R, Ma N, Kerfoot E, Wang Y et al. MONAI: An open-source framework for deep learning in healthcare. 2022.
23. Paszke A, Gross S, Massa F, Lerer A, Bradbury J, Chanan G et al. PyTorch: An Imperative Style, High-Performance Deep Learning Library. *Advances in Neural Information Processing Systems* 32. Curran Associates, Inc., 2019:8024–35.
24. Landman B, Xu Z, Igelsias J, Styner M, Langerak T, Klein A. Miccai multi-atlas labeling beyond the cranial vault—workshop and challenge. *Proc. MICCAI multi-atlas labeling beyond cranial vault—workshop challenge*. Vol. 5. Munich, Germany. 2015:12.

5 Appendix

5.1 Architectures

Figure 3, 4, 5 and 6 show schematic visualizations of the UNETR, SwinUNETR, UNETR++ and SegResNet architectures as used in this benchmark.

For UNETR, SwinUNETR and SegResNet we used the MONAI [22] implementations, which are accessible via its GitHub repository: <https://github.com/Project-MONAI/MONAI>. For UNETR++ we used the official implementation provided by the authors [5] via this github repository: https://github.com/Amshaker/unetr_plus_plus. The complete code for data preprocessing, training, testing and validation as well as the implementation of the models for this paper is available on github: https://github.com/lukas-FAU/medical_image_segmentation_benchmarking_paper.

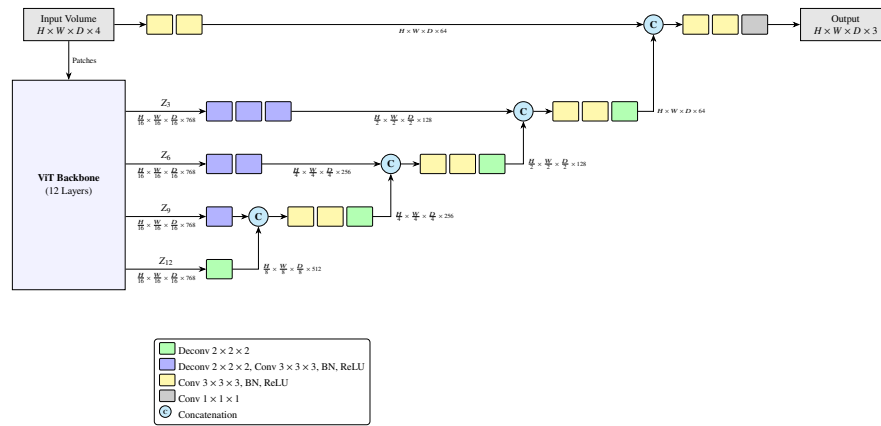


Fig. 3. Schematic visualization of the UNETR architecture as used in this benchmark. [3]

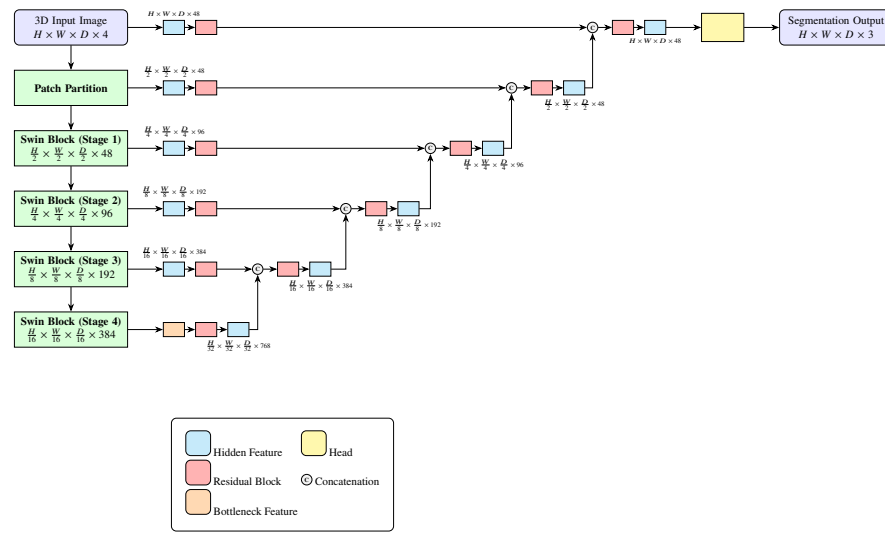


Fig. 4. Schematic visualization of the SwinUNETR architecture as used in this benchmark. [4]

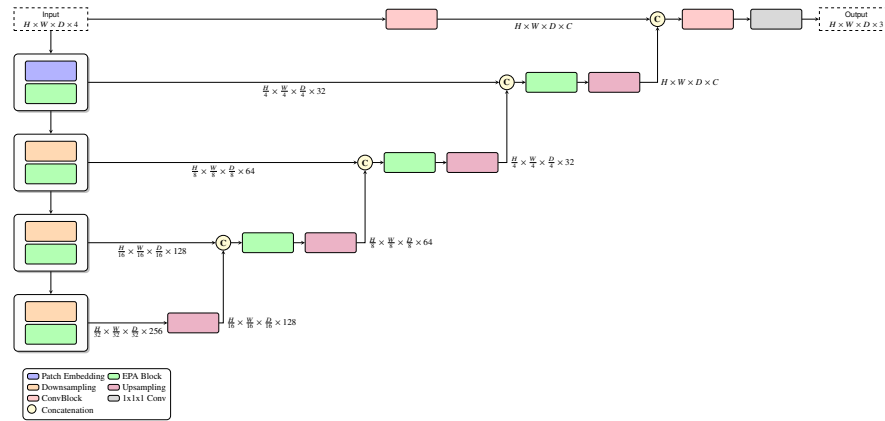


Fig. 5. Schematic visualization of the UNETR++ architecture as used in this benchmark. [5]

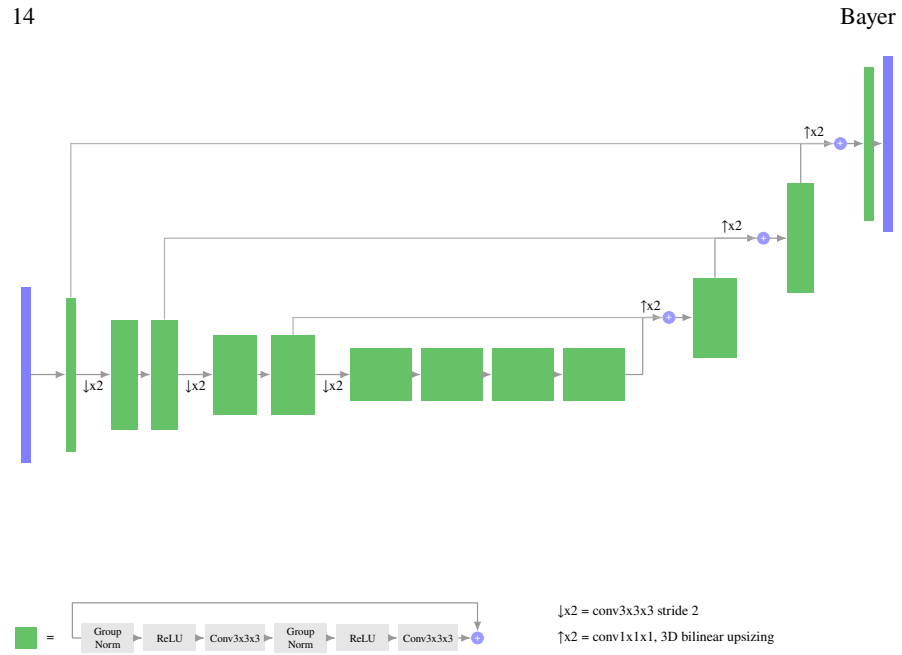


Fig. 6. Schematic visualization of the SegResNet architecture as used in this benchmark. [20]